A Self-Tuning Algorithm for Optimal QoE-Driven Traffic Steering in LTE

MARÍA LUISA MARÍ ALTOZANO[ID]**, MATÍAS TORIL**[ID]**,
SALVADOR LUNA-RAMÍREZ**[ID]**, (Member, IEEE), AND CAROLINA GIJÓN**[ID]
Department of Communication Engineering, University of Málaga, 29071 Málaga, Spain

Corresponding author: María Luisa Marí Altozano (mlma@ic.uma.es)

ABSTRACT Due to the wide diversity of services in mobile networks, cellular operators have changed their focus from Quality of Service (QoS) to Quality of Experience (QoE). To manage this change, Self-Organizing Networks (SON) techniques have been developed to automate network management, with traffic steering as a key use case. Traditionally, traffic steering aims to balance traffic volume or load among adjacent cells. Although more advanced schemes have been devised to balance QoE among cells, these do not guarantee that the overall system QoE is improved. In this work, a novel self-tuning algorithm for parameters in a classical mobility load balancing scheme is proposed to steer traffic among adjacent cells in a Long-Term Evolution (LTE) network driven by QoE criteria. Unlike previous approaches, based on heuristic rules, the proposed algorithm takes a gradient ascent approach to ensure that parameter changes always improve the overall system QoE. For this purpose, the impact of parameter changes on system QoE is estimated with an analytical network performance model that can be adjusted with statistics taken from the real network. The proposed algorithm is tested in a system-level simulator implementing a realistic LTE scenario. Results show that the method outperforms classical load and QoE mobility load balancing schemes.

I. INTRODUCTION

Over the last few years, an exponential growth in the demand of mobile services has been experienced. Due to the introduction of new services and the success of smartphones and tablets, traditional traffic patterns have substantially changed [1]. These changes will be even faster with the deployment of 5G systems, as new terminals and use cases are introduced [2]. To deal with these changes in a cost-effective manner, *Self-Organizing Networks* (SON) have been developed, consisting of a group of automation techniques for mobile network management [3], [4].

SON techniques are usually classified into three use cases: self-planning, self-healing and self-optimization [5]. Particularly, self-optimization aims to cope with user trends and traffic changes by modifying network settings. Thus, self-optimization ensures that optimal network performance is achieved along the operational stage. Traffic steering is one of the foremost self-optimization use cases [3]. The aim of traffic steering is to alleviate the negative effects of uneven traffic demand distribution by sharing traffic between adjacent cells. To this end, different objectives can be defined, amongst which is to balance some network indicator across the network (e.g., average PRB utilization [6], [7] or call blocking ratio [8]) or maximize some overall network performance figure (e.g., total blocked traffic [9] or utility function based on individual cell loads [10]). Likewise, cell re-sizing for traffic steering can be achieved by changing physical parameters (e.g., base station transmit power [11] or antenna tilt angle [12], [13]) or logical parameters (e.g., cell reselection offset [14] or HandOver (HO) margin [15], [16]). The latter is often the preferred option, since it does not affect network coverage, it is effective for connected users and can be dynamically adjusted to cope with rapid fluctuations of cellular traffic demand.

While legacy network-centric management procedures were based on system performance indicators, such as average cell throughput or accessibility ratios (a.k.a. *Quality of Service*, QoS), nowadays operators adopt user-centric approaches focused on user opinion (a k.a. *Quality of Experience*, QoE). Strictly, QoE is defined as the overall user satisfaction of a service. It is a subjective measure that depends

The associate editor coordinating the review of this manuscript and approving it for publication was Wenjie Feng.

on how the experience of the service is perceived by the user. QoE is often measured using the *Mean Opinion Score* (MOS) scale, ranging from 1 (very bad experience) to 5 (excellent experience) [17]. Due to the difficulty of measuring a subjective figure, QoE (or MOS) is computed with utility functions mapping high-level service performance indicators (e.g., packet delay for Voice-over-Internet Protocol or initial playback time for streaming services).

In the literature, several QoE-driven self-tuning algorithms for cellular networks have been proposed. For instance, a self-tuning algorithm for adjusting parameters in a dynamic packet scheduler of a LTE base station is proposed in [18] to balance QoE across services by re-prioritizing them based on service performance statistics. Closer to this work, in [19], a traffic sharing algorithm based on mobility load balancing is proposed to equalize the QoE of cells in a LTE network offering services of very different nature. For this purpose, HO margins are tuned on a per-adjacency or per-service basis based on QoE differences collected in the network management system. In [20], a data-driven traffic steering algorithm based on mobility load balancing is proposed for optimizing user experience in multi-tier LTE networks. Traffic steering is achieved by changing Reference Signal Received Quality (RSRQ) inter-frequency HO margins. The algorithm proposed there relies on an indicator showing the impact of individual HOs on user QoE, derived from connection traces.

The above-mentioned approaches formulate network tuning as a control problem. Thus, balancing algorithms are designed as controllers that tune network parameters based on heuristic rules, which makes them suitable for steering traffic in real time. However, equalizing QoE in the network does not necessarily lead to the best overall system QoE. On the contrary, it is shown in [19] that, in some cases, the worst cells (in terms of user experience) improve at the expense of degrading the global cell average QoE. This situation is avoided by formulating the tuning problem as an optimization problem, where a search algorithm evaluates the quality of different network settings and selects that maximizing the overall QoE. Following this approach, sophisticated search algorithms can be used during network planning to find the optimal configuration, provided that a network performance model is available for the QoE metric (e.g., analytical expressions [21] or a simulation tool [19]). However, in the operational stage, this search has to be performed by evaluating candidate configurations in the live network in the absence of a precise QoE model, which might degrade network performance temporarily. For safety reasons, operators prefer to modify parameters in small steps with a heuristic trajectory search method. To the authors' knowledge, no traffic steering method based on mobility load balancing explicitly considering optimality criteria for QoE has been published in the literature.

In this work, a novel self-tuning algorithm is proposed to steer traffic between cells in LTE by changing HO margins in a classical mobility load balancing scheme driven by QoE criteria. Unlike previous approaches, based on heuristic rules, the proposed approach uses a gradient ascent algorithm to ensure that changes in HO margins always improve the overall system QoE. For this purpose, the impact of small parameter changes on system QoE is estimated with an analytical network performance model that can be adjusted statistics taken from the real network. The proposed analytical approach is tested in a system-level simulator implementing a realistic macrocellular LTE scenario where users demand a file download service (*File Transfer Protocol*, FTP). The main contributions of this work are: a) a simple QoE-driven analytical optimization algorithm for tuning HO margins in LTE, and b) an analytical performance model to estimate the impact of cell re-sizing on the QoE of services that can be approximated by a full buffer traffic source. The rest of the work is organized as follows.

Section II discusses the limitations of a QoE-driven traffic steering scheme. Section III describes the analytical QoE model and optimization algorithm. Section IV presents algorithm assessment. Finally, Section V summarizes the main conclusions.

II. PROBLEM FORMULATION

In mobile networks, the HO process ensures a seamless connection between neighbor cells when the user moves. Specifically, a HO is typically triggered when the following condition is fulfilled for a time period TTT (*Time-To-Trigger*):

$$P_{rx}(j) - P_{rx}(i) \geq HOM(i, j), \qquad (1)$$

where $P_{rx}(j)$ is the pilot signal level received from neighbor cell j, $P_{rx}(i)$ is the pilot signal level received from the serving cell i, and $HOM(i, j)$ is the HO margin between cells i and j, defined on a per-adjacency basis (i.e., one value for each pair of cells and direction of the adjacency). In most cases, HO margins are set complementarily in both directions of the adjacency to prevent ping-pong effect, so that

$$HOM(i, j) + HOM(j, i) = Hyst, \qquad (2)$$

where *Hyst* represents the hysteresis value.

HO margins can be adjusted to modify cell service areas for traffic steering. Specifically, a decrease in Δ dB in $HOM(i, j)$ reduces the serving area of cell i while increasing that of cell j, so users located at the border of cell i are handed over to cell j. This cell re-sizing effect affects the QoE of all users in the surrounding area. Handed-over users are re-allocated in a different cell, experiencing different radio link signal level/quality, and different spectral efficiency. At the same time, user re-allocation causes that traffic per cell changes, causing that the amount of available radio resources for both handed-over and static users changes. Both effects might have a strong impact on individual user QoE. The above tuning problem is a large-scale non-separable optimization problem [9]. In this work, the figure of merit is the overall system QoE, defined as:

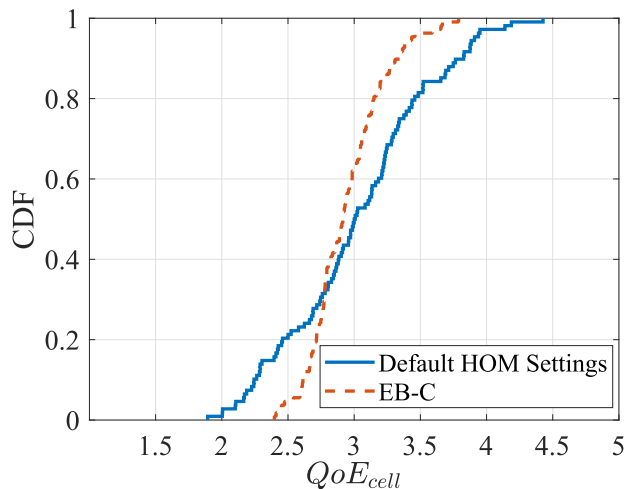$$\overline{QoE} = \frac{\sum_u QoE(u)}{N_u}, \qquad (3)$$

FIGURE 1. Cumulative distribution function of cell average QoE.

where N_u is the number of users in the system and $QoE(u)$ is the QoE experienced by each user u. The latter is given by radio link conditions of individual users, system bandwidth, cell loads and the specific dynamic packet scheduling algorithm in the base station. All these factors make that $QoE(u)$ is non-linearly related to HO margin settings, which makes the search for the optimal solution more complicated.

A first solution is to balance the average cell QoE, $QoE_{cell}(i)$, defined as

$$QoE_{cell}(i) = \frac{1}{N_u(i)} \sum_{u \in i} QoE(u) , \qquad (4)$$

where $N_u(i)$ is the number of users in cell i. Such an approach is hereafter referred to as Experience Balancing on a Cell basis (EB-C) [19]. For instance, if cell i is heavily loaded, users served by cell i are most likely unsatisfied due to a lack of radio resources. At the same time, if cell j is underutilized, users served by cell j are most likely satisfied due to overprovisioning. In this situation, a QoE balancing algorithm decreases $HOM(i, j)$, so that users from cell i are handed over to cell j, leading to a more fairly distributed user satisfaction between both cells. As a result, users in cell i experiencing worst QoE see their experience improved at the expense of degrading the experience of those in cell j with the highest QoE.

Figure 1 presents an example of how QoE is affected by EB-C, showing the cumulative distribution function of the global (i.e., network-wide) QoE distribution per cell before/after equalizing the QoE. It is observed that traffic steering improves cells with worst average QoE at the expense of degrading the best cells. Thus, a more balanced QoE distribution is obtained, but the overall system QoE is degraded, which can be inferred from the shift of the median value to the left. By enforcing that all cells have the same QoE, highly loaded cells are prioritized over low loaded cells. However, in the example, the QoE increase in the former cells is lower than the QoE decrease in the latter. Alternatively, changes in HO margins can be driven

by optimality criteria provided that a network performance model is available. Unfortunately, the large number of factors influencing QoE makes that only approximate analytical models can be derived. Nonetheless, should the approximate model be able to find reasonable estimates of the gradient of the objective function, a gradient ascent algorithm can be used to progressively improve the overall figure for merit. Thus, a local maximum of the problem can be achieved. Equally important, the gradient rule ensures that no parameter change degrades system performance if the magnitude of changes is small.

III. OPTIMIZATION ALGORITHM

The proposed QoE-driven optimization algorithm, hereafter referred to as OE (for Optimizing Experience), modifies the HO margin between neighbor cells i and j, $HOM(i, j)$, with the aim of maximizing overall system QoE, $\overline{QoE}$. For this purpose, OE follows a gradient ascent approach, where an iterative algorithm changes $HOM(i, j)$ based on estimates of the gradient of the objective function, $\overline{QoE}$, computed on an adjacency basis with an analytical model. In each iteration (optimization loop), HO margins in all adjacencies are updated as

$$HOM^{(n+1)}(i, j) = HOM^{(n)}(i, j) + \Delta HOM^{(n)}(i, j)$$
$$= HOM^{(n)}(i, j) + f\left(\frac{\delta \overline{QoE}}{\delta HOM(i, j)}\right)^{(n)}, \qquad (5)$$

where superscripts (n) and $(n + 1)$ denote the optimization loop index, and $\frac{\delta \overline{QoE}}{\delta HOM(i,j)}$ is the gradient of the objective function in the direction of the decision variable $HOM(i, j)$, quantifying the impact of increasing HOM in an adjacency on the overall system QoE. The resulting HOM values are bounded in the interval $[-7, 13]$ dB to ensure a minimum signal quality after HO [22]. The lower limit is the minimum signal-to-interference-plus-noise ratio (SINR) needed for the scheduler to assign any radio resource to a connection in most vendors. The upper limit is calculated with (2) to ensure a hysteresis level of $Hyst = 6$ dB. $\Delta HOM^{(n)}(i, j)$ is the value to be estimated with the analytical model described next.

A. ANALYTICAL SYSTEM MODEL FOR OPTIMIZATION

The aim of the optimization algorithm is to maximize the overall system QoE. To this end, an analytical model is developed to compute gradient estimates of the objective function. For simplicity, it is assumed here that all users demand FTP service, which can be modeled as a full buffer traffic source until session ends. Yet, it is considered that user experience depends on user context (indoors or outdoors), which can be inferred by analyzing connection traces in practice [23]. Thus, two utility functions are used, depending on user location [24]. For *outdoor* users, QoE is estimated as

$$QoE_{outdoor}^{(FTP)}(u) = \max(1, \min(5, 6.5TH(u) - 0.54)) , \quad (6)$$

where *TH* is the average user throughput in Mbps. For *indoor* users, QoE is estimated as

$$QoE_{indoor}^{(FTP)}(u) = \max\left(1, \min\left(5, 6.5\frac{TH(u)}{1.5} - 0.54\right)\right) . \quad (7)$$
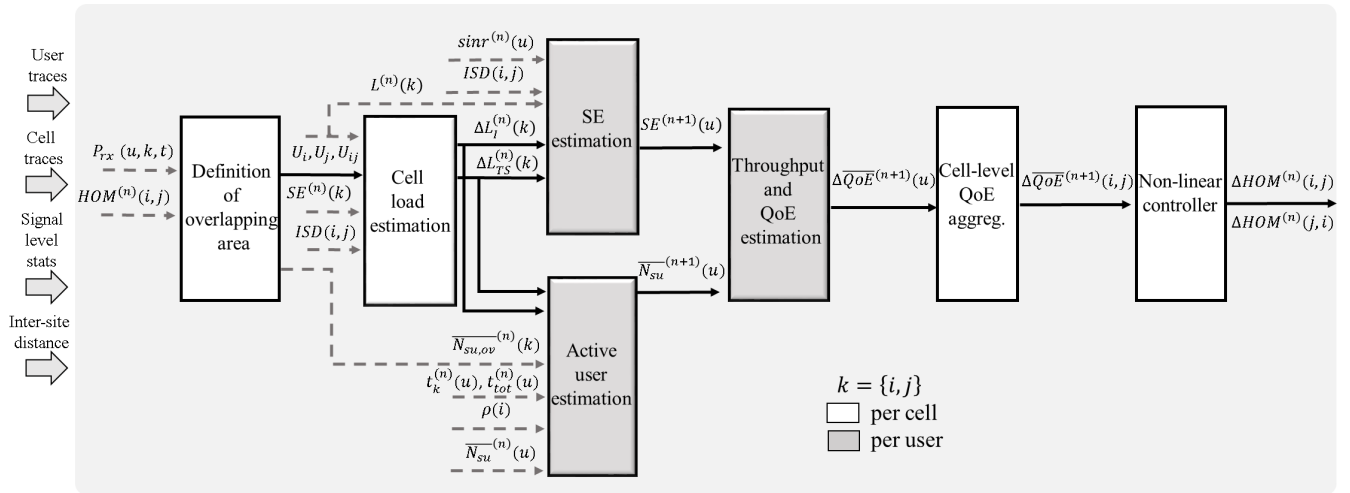
FIGURE 2. Flow diagram of the computation of changes in handover margins per adjacency.

In (6)-(7), QoE is limited to the MOS scale (1 to 5). By comparing (6) and (7), it is observed that, in the latter, *TH* is divided by 1.5, reflecting that indoor users experience worse QoE for the same *TH* value, since expectations of indoor users are higher.

In the above utility functions, user QoE only depends on *TH*. Thus, the analytical model must only establish the relationship between HOM and *TH* changes, which can then be translated into QoE changes. Specifically, the gradient of the objective function is computed on an adjacency basis by aggregating the impact of changes across users in the adjacency as

$$\frac{\delta \overline{QoE}}{\delta HOM(i,j)}$$
$$= \sum_u \frac{\delta QoE(u)}{\delta HOM(i,j)}$$
$$= \sum_u [\frac{\delta QoE(u)}{\delta TH(u)} \frac{\delta TH(u)}{\delta SE(u)} \frac{\delta SE(u)}{\delta SINR(u)} \frac{\delta SINR(u)}{\delta HOM(i,j)}$$
$$+ \frac{\delta QoE(u)}{\delta TH(u)} \frac{\delta TH(u)}{\delta BW(u)} \frac{\delta BW(u)}{\delta N_{su}(k)} \frac{\delta N_{su}(k)}{\delta A(k)} \frac{\delta A(k)}{\delta HOM(i,j)}], \quad (8)$$

where k is the cell serving user u (i.e., cell i or j), $BW(u)$ is the average system bandwidth assigned to the user, $N_{su}(k)$ is the average number of simultaneous active users with user u in the cell serving (excluding inactive periods), $A(k)$ is the service area of cell k, and $SE(u)$ and $SINR(u)$ are the average spectral efficiency and signal quality of user u.

The chain rule in (8) reflects that any user throughput change achieved by traffic sharing is due to: a) a change in radio link conditions (experienced, e.g., by a user re-allocated in a new cell), or b) a change in the number of available resources for the user caused by the new number of simultaneous users in the cell (originated, e.g., by the new cell size or the change of serving cell). To increase the robustness of the method, the gradient is approximated by estimating the impact of a large change in the HO margin of the adjacency under study (i.e., 3 dB) on the overall system

QoE, $\Delta \overline{QoE}$. Such a large perturbation allows to anticipate effects that could not be observed with smaller changes (e.g., 1 dB).

Figure 2 shows a flow diagram of the proposed algorithm, whose aim is to estimate the potential impact of traffic sharing on QoE at a connection level, which is then aggregated at a cell level to derive HO margin changes per adjacency. The inputs to the method are: a) user traces, including performance measurements at a connection level, b) cell traces, including instantaneous performance measurements at a cell level, c) signal level statistics, including reference signal measurements from serving and neighbor cells, and d) Inter-Site Distance (ISD), computed from site coordinates. The output is the change in HO margin in the adjacency. For clarity, variables directly taken from measurements are depicted with dashed lines, to isolate them from estimated variables, shown with solid lines. Likewise, stages (i.e., boxes in the figure) dealing with cell-level stats are filled in white and stages dealing with connection-level stats are filled in gray. Hereafter, for brevity, k denotes both source and target cell in the adjacency, i and j. All stages in the figure are described next.

1) DEFINITION OF OVERLAPPING AREA
A first step is to estimate the amount of traffic re-allocated by changing the HO margin. To this end, users (connections) in cells i and j are classified into three sets, depending on whether they change serving cell due to traffic sharing. On the one hand, U_i and U_j denote the part of connections in cell i and j that keep served by i and j after traffic sharing. On the other hand, U_{ij} denotes the part of connections that would be re-allocated by the traffic sharing algorithm. As in [25], U_{ij} is identified precisely from pilot signal level statistics collected by base stations, as those users u fulfilling that

$$P_{rx}(u,j,t) \geq P_{rx}(u,i,t) + HOM(i,j) - 3, \quad j \neq i, \quad (9)$$

where $P_{rx}(u,i,t)$ is the Reference Signal Received Power (RSRP) received by user u from cell i at time t.

By aggregating the time these users are in the overlapping area between adjacent cells, the method computes the average number of simultaneous connections removed by traffic steering in active periods of cell i, $\overline{N_{su,ov}}^{(n)}(i)$. The number of connections removed by traffic steering in active periods of cell j is computed in the same way but interchanging the index of cells i and j.

2) CELL LOAD ESTIMATION

In this stage, changes in the average load in cell i and j load are estimated. The inputs to this stage are the sets of users, $U_x(x \in \{i, j, ij\})$, the average cell load and spectral efficiency before changes, $L^{(n)}(k)$ and $SE^{(n)}(k)$, and the ISD in the adjacency, $ISD(i, j)$. The main output of this stage are the new cell loads after traffic sharing.

If users in the overlapping area are handed over from cell i to cell j, the load of cell i decreases and that of cell j increases. However, at the same time, the interference from cell j received in cell i increases due to the load increase in the former. Thus, the spectral efficiency of cell i might decrease, causing an increase of cell load that might counteract the congestion relief effect of traffic steering. The contrary effect is observed in the spectral efficiency of cell j. To model both effects, load changes are broken down in two components as

$$\Delta L^{(n)}(k) = \Delta L_{TS}^{(n)}(k) + \Delta L_I^{(n)}(k), \quad k \in \{i, j\}, \quad (10)$$

where $\Delta L_{TS}^{(n)}(k)$ reflects the change due to the different number of users caused by the HO of users from cell i to cell j, and $\Delta L_I^{(n)}(k)$ reflects the change due to the different signal quality (spectral efficiency) caused by the new interference conditions.

Specifically, the load change in source cell i due to traffic steering is calculated as

$$\Delta L_{TS}^{(n)}(i) = -\sum_{u_{ij}} \Delta L^{(n)}(u_{ij}, i), \quad (11)$$

where $L^{(n)}(u_{ij}, i)$ is the PRB utilization ratio removed from cell i by steering user u_{ij} to cell j, derived from the total connection time in the overlapping area observed in signal level measurements. Then, the load change in the target cell j due to traffic steering is estimated by rescaling the load removed from the source cell by considering the spectral efficiency in both cells as

$$\Delta L_{TS}^{(n)}(j) = \Delta L_{TS}^{(n)}(i)\frac{SE^{(n)}(i)}{SE^{(n)}(j)}. \quad (12)$$

Load changes due to interference are estimated depending on Inter-Site Distance to differentiate between interference-limited and noise-limited scenarios. In the source cell, the interference-related term is estimated as

$$\Delta L_I^{(n)}(i)$$
$$= \begin{cases} L^{(n)}(i)\left[\dfrac{SE^{(n)}(i)}{SE^{(n+1)}(i)} - 1\right] & \text{if } ISD(i, j) \leq 1.25 \text{ km,} \\ 0 & \text{otherwise,} \end{cases}$$
$$(13)$$

where $SE^{(n)}(i)$ is the average spectral efficiency of cell i measured at loop n, and $SE^{(n+1)}(i)$ is the average spectral efficiency of cell i at loop $n+1$. In the latter, it is assumed that interference is much larger than noise (interference-limited scenario) and all interference received in cell i comes from cell j (single interferer), so that

$$SE^{(n+1)}(i) = SE^{(n)}(i)\frac{L^{(n)}(j)}{L^{(n)}(j) + \Delta L_{TS}^{(n)}(j)}. \quad (14)$$

Similarly, the interference-related term in the target cell is estimated as

$$\Delta L_I^{(n)}(j)$$
$$= \begin{cases} L^{(n)}(j)\left[\dfrac{SE^{(n)}(j)}{SE^{(n+1)}(j)} - 1\right] & \text{if } ISD(i, j) \leq 1.25 \text{ km,} \\ 0 & \text{otherwise,} \end{cases}$$
$$(15)$$

where

$$SE^{(n+1)}(j) = SE^{(n)}(j)\frac{L^{(n)}(i)}{L^{(n)}(i) + \Delta L_{TS}^{(n)}(i)}. \quad (16)$$

It should be pointed out that the single-interferer assumption in (13) and (15) is the worst case of interference-limited scenarios where traffic steering achieves the lowest congestion relief effect. Results presented later show that such an approximation has a negligible impact on method performance.

3) SPECTRAL EFFICIENCY ESTIMATION

The next stage is to estimate changes in spectral efficiency per user. The input to this stage is the SINR per user $sinr^{(n)}(u)$, the ISD between cell i and cell j, $ISD(i, j)$, the average cell load before changes, $L^{(n)}(k)$, and the estimation of cell load changes $\Delta L_{TS}^{(n)}(k)$ and $\Delta L_I^{(n)}(k)$. The output is the estimated spectral efficiency for the next loop per user, $SE^{(n+1)}(u)$. This estimation is carried out on a user basis only if the distance from cell i to cell j is less than 1.25 km. Under these circumstances, it can be assumed that interference I received from adjacent cell j is much greater than noise, so that $sinr^{(n)}(u) \simeq \frac{c}{i}^{(n)}(u)$, $\forall u \in \{U_i, U_j, U_{ij}\}$. Otherwise, spectral efficiency remains invariant. Specifically, for users served by cell i, spectral efficiency is estimated as

$$SE^{(n+1)}(u_i)$$
$$\simeq \begin{cases} \log_2(1 + \dfrac{c}{i}^{(n)}(u_i)\dfrac{L^{(n)}(j)}{L^{(n+1)}(j)}) & \text{if } ISD(i, j) \leq 1.25 \text{ km,} \\ SE^{(n)}(u_i) & \text{otherwise,} \end{cases}$$
$$(17)$$

where the factor $\frac{L^{(n+1)}(j)}{L^{(n)}(j)}$ reflects the increase in interference (decrease in signal quality) due to neighbor cell load increase. Note that cell load estimation for next iteration $L^{(n+1)}(k)$ can be easily calculated from the estimation of cell load changes as

$$L^{(n+1)}(k) = L^{(n)}(k) + \Delta L_{TS}^{(n)}(k) + \Delta L_I^{(n)}(k). \quad (18)$$

Similarly, for users served by cell j, spectral efficiency is estimated as

$$SE^{(n+1)}(u_j)$$
$$\simeq \begin{cases} \log_2(1 + \dfrac{c^{(n)}}{i}(u_j)\dfrac{L^{(n)}(i)}{L^{(n+1)}(i)})) & \text{if } ISD(i,j) \leq 1.25 \text{ km,} \\ SE^{(n)}(u_j) & \text{otherwise.} \end{cases}$$
$$(19)$$

Finally, for users in the overlapping area, spectral efficiency is estimated as

$$SE^{(n+1)}(u_{ij}) \simeq \begin{cases} SE^{(n)}(u_{ij}(j)) & \text{if } u_{ij}(j) \neq 0, \\ SE^{(n)}(u_{ij}(j)) & \forall u_{ij}(j) \neq 0 \text{ otherwise,} \end{cases} \quad (20)$$

where users in the overlapping area are divided in two different groups: those who were handed over from cell i to cell j in the optimization loop n, $u_{ij}(j) \neq 0$, and those who were not $u_{ij}(j) = 0$.

4) ACTIVE USER ESTIMATION

The fourth stage addresses the number of simultaneous users in the next loop. A preliminary analysis (not presented here) shows that this variable has to be estimated on a per-user basis to obtain reliable estimates of user throughput and QoE. The input to this stage are the estimation of cell load changes, together with the average number of simultaneous users in the overlapping area during active periods, $\overline{N_{su,ov}}^{(n)}(i)$, the time spent by the user in cell $k = \{i, j\}$, $t_k^{(n)}(u)$, the total connection duration, $t_{tot}^{(n)}(u)$, the activity ratio of cell i (measured as the ratio of active TTIs), $\rho(i)$, and the average number of simultaneous users when each user is transmitting in the current loop, $\overline{N_{su}}^{(n)}(u)$. The output is the number of active users with each user, $\overline{N_{su}}^{(n+1)}(u)$.

The expected number of simultaneous users in source cell i in the next loop for a user u is calculated from the value in the past loop as

$$\overline{N_{su}}^{(n+1)}(u_i) = \overline{N_{su}}^{(n)}(u_i) - \overline{N_{su,ov}}^{(n)}(i) + \overline{\Delta N_{su,I}}^{(n)}(i),$$
$$(21)$$

where $\overline{N_{su,ov}}^{(n)}(i)$ captures the decrease in the number of active users due to congestion relief achieved by handing over users, and $\overline{N_{su,I}}^{(n)}(i)$ reflects the increase in the number of active users due to the loss of spectral efficiency from a higher interference. Note that, by definition, the former quantities are measured considering only periods of cell activity (i.e., $\overline{N_{su}}^{(n)}(u_i) \geq 1$). For the same reason, $\overline{N_{su,ov}}^{(n)}(i)$ and $\overline{N_{su,I}}^{(n)}(i)$ are measured considering only periods of cell activity in cell i. To estimate $\overline{N_{su,I}}^{(n)}(i)$, a empirical regression analysis is performed to find the expression relating cell load L with the number of active users N_{su} in a cell, $N_{su}(L)$. In practice, such an analysis can easily be done with performance counters aggregated at a cell level stored in the network management system. In this work, this analysis is carried out by simulations. The resulting regression curve is

the exponential function

$$N_{su}(L) = 1.851 e^{1.505L}. \quad (22)$$

The sensitivity in the number of active users due to increments of cell load is obtained by derivating the above exponential function, as

$$\frac{\delta N_{su}}{\delta L}(L) = 1.851 \cdot 1.505 e^{1.505L}. \quad (23)$$

The latter is used to quantify the increase in the number of active users due to interference from the increase of cell load due to traffic steering, $\Delta L_{TS}^{(n)}(i)$, and interference, $\Delta L_I^{(n)}(i)$, as

$$\overline{\Delta N_{su,I}}^{(n)}(i) = \Delta L_I^{(n)}(i) \frac{\Delta N_{su}}{\Delta L}(L^{(n)}(i) + \Delta L_{TS}^{(n)}(i)). \quad (24)$$

Note that changes in the number of users in source cell i due to traffic steering (i.e., users in the overlapping area) can be directly taken from network measurements. In contrast, changes in target cell j have to be estimated. For this purpose, it must be taken into account that handed-over users might require a different amount of resources in the new cell, because of new radio link conditions. This can easily be taken into account by multiplying by the ratio of the average cell spectral efficiency in the old and target cell. To account for this effect, the new average number of active users in target cell j is estimated as

$$\overline{N_{su}}^{(n+1)}(u_j) = \overline{N_{su}}^{(n)}(u_j)$$
$$- \overline{N_{su,ov}}^{(n)}(i)\rho(i)\frac{SE^{(n)}(i)}{SE^{(n)}(j)} + \overline{\Delta N_{su,I}}^{(n)}(j),$$
$$(25)$$

following the same structure as (21). $\rho(i)$ is the activity ratio of cell i (measured as the ratio of active Time transmission Intervals, TTIs). Similarly to (24), $\overline{\Delta N_{su,I}}^{(n)}(j)$ is estimated as

$$\overline{\Delta N_{su,I}}^{(n)}(j) = \Delta L_I^{(n)}(j) \frac{\Delta N_{su}}{\Delta L}(L^{(n)}(j) + \Delta L_{TS}^{(n)}(j)), \quad (26)$$

using the same derivative function as that in (23). Finally, for users in the overlapping area u_{ij} that already performed HO from i to j in the previous loop (without traffic steering), the number of simultaneous users in loop $n+1$ is estimated as a weighted average of the measured number of simultaneous users during the segments of the connections in cell i and j in the previous loop, u_i and u_j, weighted by the time in each cell i and j, as

$$\overline{N_{su}}^{(n+1)}(u_{ij}) = \frac{t_i^{(n)}(u_{ij})}{t_{tot}^{(n)}(u_{ij})}\overline{N_{su}}^{(n+1)}(u_i) + \frac{t_j^{(n)}(u_{ij})}{t_{tot}^{(n)}(u_{ij})}\overline{N_{su}}^{(n+1)}(u_j),$$
$$(27)$$

where $t_i^{(n)}(u_{ij})$ and $t_j^{(n)}(u_{ij})$ is the time that user u_{ij} spent in cells i and j, respectively, and $t_{tot}^{(n)}(u_{ij})$ is the total time user u is served by both cells.

5) THROUGHPUT AND QOE ESTIMATION

Once the number of simultaneous users with every user in the network has been estimated for the next optimization loop $n + 1$, $\overline{N_{su}}^{(n+1)}(u)$, as well as the spectral efficiency, $SE^{(n+1)}(u)$, the output to this stage is the best HOM variation $\Delta QoE^{(n+1)}(u)$. For it, user throughput variations will be estimated first, then, QoE changes on a user basis.

The estimation of user throughput after a HOM change is then calculated as usual as

$$
\begin{aligned}
TH^{(n+1)}(u) &= SE^{(n+1)}(u)BW^{(n+1)}(u) \\
&= SE^{(n+1)}(u)\frac{N_{PRB}}{\overline{N_{su}}^{(n+1)}(u)}, \quad \forall u \in U_i, U_j, U_{ij},
\end{aligned}
\tag{28}
$$

where N_{PRB} is the system bandwidth and $SE^{(n+1)}(u)$ is considered as throughput per PRB.

Throughput values are easily translated into QoE with (6)-(7). Then, the change in user QoE due to HOM changes is estimated as

$$
\Delta QoE^{(n+1)}(u) = QoE^{(n+1)}(u) - QoE^{(n)}(u),
$$
$$
\forall u \in U_i, U_j, U_{ij}.
\tag{29}
$$

6) CELL LEVEL QOE AGGREGATION

The network average QoE variation due to $HOM(i, j)$ modification is calculated as

$$
\Delta QoE^{(n+1)}(i, j) = \frac{\sum\limits_{u \in U_i, U_j, U_{ij}} \Delta QoE^{(n+1)}(u)}{N_u(i) + N_u(j)},
\tag{30}
$$

i.e., the aggregation of every individual QoE modification divided by the number of users in cells i and j (which is maintained in iterations n and $n + 1$).

The above analysis considers the case when $HOM(i, j)$ is decreased. The opposite case, when $HOM(i, j)$ is increased, can be evaluated by analyzing the opposite side of the adjacency, where $HOM(j, i)$ is decreased to satisfy (2). The whole estimation process explained above must be repeated for a similar decrease of $HOM(j, i)$ by 3 dB, getting $\Delta QoE^{(n+1)}(j, i)$ estimation. Therefore, two estimations of average QoE variations are obtained per adjacency: $\Delta QoE^{(n+1)}(i, j)$ and $\Delta QoE^{(n+1)}(j, i)$, corresponding to both HOM movements, i.e., reducing cell i or j service areas, respectively. OE algorithm discerns which option obtains the highest ΔQoE value (i.e., move traffic from cell i to j, or viceversa). If both movements degrade the overall QoE in the adjacency, no HOM change is made (gradient ascent rule).

7) NON-LINEAR CONTROLLER

Finally, to define the magnitude of HOM changes, the incremental controller shown in Figure 3 is used. It is observed that the controller includes a gain scheduling algorithm modifying the feedback loop gain to control the trade-off between convergence speed and system stability. A coring operation ensures that no changes are implemented when expected QoE benefits are below 0.01. Thus, the control system reaches
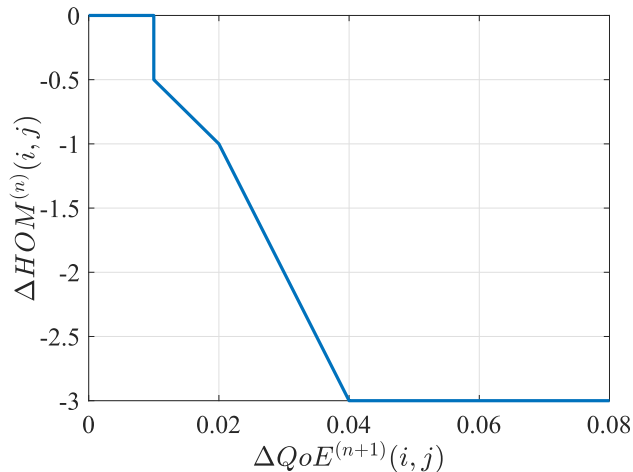

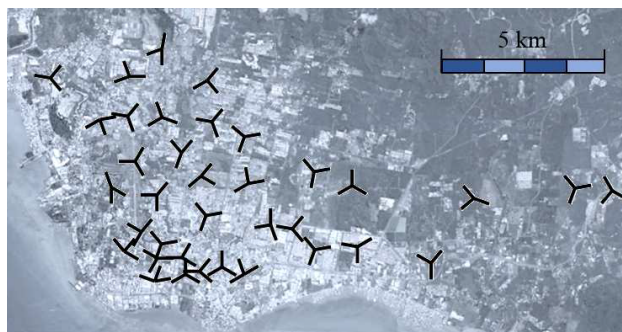**FIGURE 3.** Proportional controller per adjacency (i, j).

FIGURE 4. Simulated scenario.

equilibrium earlier. Beyond that value, a larger slope is used to favor adjacencies with larger expected QoE benefits. To avoid instabilities, the maximum HOM change per iteration is limited to 3 dB.

The figure shows the case when $\Delta QoE^{(n+1)}(i, j) > 0$ and $\Delta QoE^{(n+1)}(i, j) > \Delta QoE^{(n+1)}(j, i)$ (i.e., decreasing $HOM(i, j)$ is more beneficial than decreasing $HOM(j, i)$). In this case, the controller computes the HOM change in adjacency (i, j), $\Delta HOM^{(n)}(i, j)$, so that $HOM^{(n+1)}(i, j) = HOM^{(n)}(i, j) + \Delta HOM^{(n)}(i, j)$. To maintain hysteresis, $HOM^{(n+1)}(j, i) = HOM^{(n)}(j, i) - \Delta HOM^{(n)}(i, j)$. In the opposite scenario (i.e., decreasing $HOM(j, i)$ is more beneficial than decreasing $HOM(i, j)$), the controller works the same, just interchanging indexes i and j.

IV. PERFORMANCE ANALYSIS

In this section, the proposed optimization algorithm is validated with simulations. For clarity, the simulation tool and analysis methodology are first presented, and results are shown later. Finally, implementation issues are discussed.

A. SIMULATION TOOL

Figure 4 shows the simulated scenario, consisting of 108 macrocells (36 sites with 3 tri-sectorized antennas per site) covering a seamless area of 60 km² [19]. Table 1 presents its main parameters.

TABLE 1. Main simulation parameters.

Time resolution	10 TTI (10 ms)
Propagation model	Pathloss COST 231 Okumura-Hata, slow fading (log-normal σ = 8 dB, d_{corr} = 20 m), fast fading (ETU model)
Base station model	Tri-sectorized antennas, MIMO 2x2, BW = 5 MHz (25 PRB), $f_{carrier}$ = 1850 MHz, EIRP$_{max}$= 67 dBm.
Traffic model	Based on live statistics collected on a cell basis
Mobility model	Random direction, constant speed, 3 km/h.
Radio resource management model	Scheduler: *Classical exponential/Proportional fair* [26]
Link adaptation	CQI-based

The FTP traffic model reflects the download a file whose size follows a log-normal distribution of average 2 MB. FTP has been chosen as it is representative of a full-buffer service.

The simulation tool includes two types of users: indoor and outdoor. Indoor users are static users with higher demands in terms of QoE, even if propagation losses are 15 dB higher than those of the outdoor users. Outdoor users move at 3 km/h following a random straight path. The percentage of indoor users per cell depends on cell location. For this purpose, 36 % of cells are categorized as urban, 46 % as suburban and 18 % as rural, based on the predominant land use in its service areas. Then, it is assumed that urban cells have 70 % of indoor users, sub-urban cells have 50 % of indoor users and rural cells have 10 % of indoor users. The overall traffic demand is controlled by adjusting the total mean call arrival rate in the scenario so as to generate load (and QoE) congestion problems. Spatial traffic distribution at a cell level follows the same profile as in the live network. With default HOM settings, the average cell load in the network is $\overline{U(i)} = 61$ %. Nonetheless, the minimum and maximum cell loads in the scenario are 3.5 % and 100 %, respectively, showing that traffic demand is unevenly distributed.

B. ANALYSIS METHODOLOGY

Four iterative self-tuning methods are compared. The first three are balancing algorithms that aim to equalize some indicator between neighbor cells by adjusting HOM on an adjacency basis, and they are used with comparison purposes. A first method is a classical mobility Load Balancing (LB) algorithm that seeks to solve local congestion problems by equalizing average PRB utilization. A second method is a Throughput Balancing (TB) algorithm, equalizing average user throughput between adjacent cells [27]. A third method is a QoE balancing algorithm (EB-C), conceived to solve user experience problems by equalizing average cell QoE [19]. Parameter tuning in LB, TB and EB-C is carried out by fuzzy logic controllers implementing simple 'IF-THEN' control rules. The fourth method is the proposed QoE-driven analytical optimization algorithm (OE). For all algorithms, 14 optimization loops of 30 minutes of network time are simulated. To assess the methods, the main figure of merit is the overall system QoE, $\overline{QoE}$, defined in (3). For a more

detailed analysis, the average deviation from HOM default settings is also computed per iteration as

$$\overline{HOM^{(dev)}}^{(n)} = \frac{\sum_{\forall i} \sum_{\forall j \neq i} HOM^{(n)}(i,j) - HOM^{(0)}(i,j)}{N_{adjs}}, \quad (31)$$

where $HOM^{(n)}(i,j)$ and $HOM^{(0)}(i,j)$ are HOM values for the adjacency (i,j) in the optimization loop n and 0 (i.e., initial state with default settings), respectively, and N_{adjs} is the number of adjacencies in the scenario. In this work, $HOM^{(0)}(i,j) = 3$ dB for all adjacencies.

Moreover, three indicators are used to check the ability of methods to balance a particular indicator by checking performance differences between neighbor cells across the network. An average load imbalance indicator $\overline{U_{imb}}$ is defined as

$$\overline{U_{imb}} = \frac{1}{N_c} \sum_{\forall i} |U_{imb}(i)| = \frac{1}{N_c} \sum_i \left| U(i) - \frac{\sum_{j \in A(i)} U(j)}{N_{adjs}(i)} \right|, \quad (32)$$

where N_c is the number of cells in the scenario, $N_{adjs}(i)$ is the number of adjacent cells for cell i and $A(i)$ is the set of adjacent cells for cell i. Similarly, an average cell QoE imbalance indicators is defined as [19]

$$\overline{QoE_{cell,imb}} = \frac{1}{N_c} \sum_i \left| QoE_{cell,imb}(i) \right|$$

$$= \frac{1}{N_c} \sum_i \left| QoE_{cell}(i) - \frac{\sum_{j \in A(i)} QoE_{cell}(j)}{N_{adjs}(i)} \right|. \quad (33)$$

Finally, an average cell throughput imbalance indicator is defined as (34)

$$\overline{TH_{imb}} = \frac{1}{N_c} \sum_i |TH_{imb}(i)|$$

$$= \frac{1}{N_c} \sum_i \left| TH(i) - \frac{\sum_{j \in A(i)} TH(j)}{N_{adjs}(i)} \right|. \quad (34)$$

C. RESULTS

Figure 5 shows the evolution of the overall system QoE with the four approaches along the 14 optimization loops. It is observed that $\overline{QoE}$ with OE is clearly different from that achieved with the three balancing algorithms, LB, TB and EB-C. In the initial state, with a HOM value of 3 dB for all adjacencies, $\overline{QoE} = 3.08$. At the end of the tuning process, OE achieves $\overline{QoE} = 3.3$, versus 2.56, 2.48 and 2.63 for LB, TB and EB-C, i.e., around 0.6 MOS points higher than the second best algorithm (EB-C). More importantly, OE manages to increase $\overline{QoE}$ by 0.2 MOS points compared to its initial state (3.3 versus 3.08), while other approaches decrease $\overline{QoE}$ by 0.52, 0.6 and 0.43 MOS points, respectively. As expected, OE reaches best $\overline{QoE}$ figures due to its analytical formulation that considers signal, congestion and interference issues, and considers optimality.
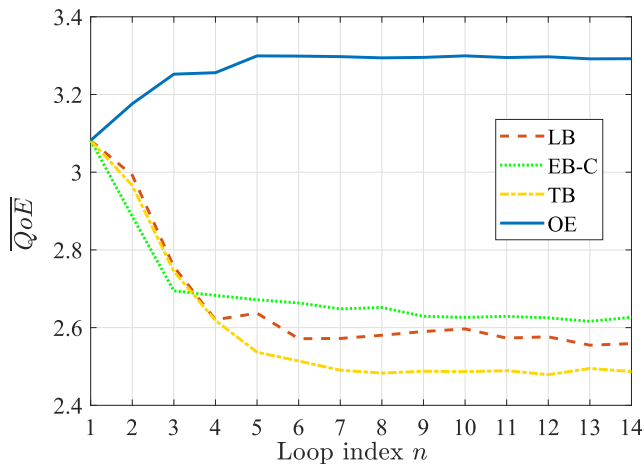
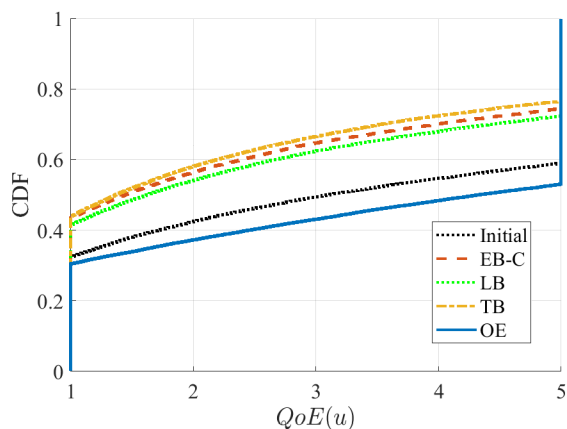**FIGURE 5.** Evolution of $\overline{QoE}$.

FIGURE 6. Cumulative distribution function of user QoE.

Equally important, the overall improvement in user QoE is not achieved at the expense of deteriorating the QoE of the worst users. To confirm this statement, Figure 6 compares the cumulative distribution function of user QoE in the scenario obtained by the methods against that with default settings (initial curve). In the initial situation, a significant share of users (35 %) have the lowest possible QoE ($QoE(u) = 1$), even if also many of them (40 %) have the highest QoE ($QoE(u) = 1$). This is due to the large mean call arrival rate and uneven spatial traffic distribution in the scenario. Unexpectedly, it is observed that balancing algorithms designed to equalize performance at a cell level increase the share of bad users. A closer analysis (not presented here) shows that LB and TB try to equalize traffic indicators without considering the service mix. Likewise, EB-C does not improve the average user QoE because when balancing $QoE_{cell}(i)$ it improves the worst users at the worst cells at the expense of degrading users experiencing better QoE in their neighbor cells. In contrast, OE reduces the number of completely unsatisfied users from 35 to 30 %, while also increasing the number of fully satisfied users from 41 to 42 %. Most percentiles of the distribution maintain these differences. For instance, the 35th percentile of $QoE(u)$ is

TABLE 2. Main performance indicators.

	Initial	LB	TB	EB-C	OE
$\overline{U_{imb}}$ [%]	18.84	7.43	10.3	11.22	15.14
$\overline{TH_{imb}}$ [Mbps]	0.90	0.36	0.22	0.36	0.85
$\overline{QoE_{cell,imb}}$	0.71	0.55	0.3	0.53	0.71
$\overline{QoE}$	3.08	2.56	2.48	2.63	3.3
$\overline{QoE_{cell}}$	3.73	2.62	2.64	2.88	3.84

1.22 in the initial configuration with default HOM settings, 1 for LB, EB-C and TB, and 1.65 for OE.

Table 2 shows all performance indicators for the *initial* state and at the end of the optimization process for the tested algorithms (columns LB, TB, EB-C and OE). For clarity, the best algorithm per indicator is highlighted in gray. As expected, $\overline{U_{imb}(i)}$, $\overline{TH_{imb}}$ and $\overline{QoE}$ reach their best performance with those approaches for which were designed (i.e., LB, TB and OE, respectively). In particular, LB achieves the lowest average cell load imbalance, i.e., $\overline{U_{imb}} = 7.43$ % and TB achieves the lowest throughput imbalance, $\overline{TH_{imb}} = 0.22$ Mbps.

However, surprisingly, the lowest $\overline{QoE_{cell,imb}}$ is achieved by TB ($\overline{QoE_{cell,imb}} = 0.3$), and not with EB-C ($\overline{QoE_{cell,imb}} = 0.53$), at the expense of a higher degradation of $\overline{QoE_{cell}}$ (2.64 against 2.88 for TB and EB-C, respectively). This unexpected behavior is due to the limits of the QoE utility functions (6)-(7), reaching saturation values (QoE = 1 or 5) with very different $TH(u)$ values (0.237 and 0.853 Mbps, respectively, for *outdoor* users). Very different $TH(i)$ and $TH(j)$ values can coexist with similar average cell QoE, $QoE_{cell}(i)$ and $QoE_{cell}(j)$ (e.g., two cells with $TH(i) = 0.05$ Mbps and $TH(j) = 0.26$ Mbps on average would experience $QoE_{cell}(i) = 1$ and $QoE_{cell}(j) = 1.1$, respectively). Under these circumstances, while there is a minimum QoE difference between them, there is a high cell average throughput difference. Therefore, TB continues operating by degrading $QoE_{cell}(j)$, while $\overline{QoE_{cell,imb}}$ keeps improving (i.e., 0.3). Thereby $\overline{QoE_{cell}}$ achieved by EB-C is 0.24 MOS points higher than that of TB. When mixing different services using different utility functions to compute QoE, the relationship between throughput and QoE is not so limited as in this scenario, and both aims (balancing $TH(i)$ and $QoE_{cell}(i)$) would follow different optimization trajectories [19].

Figure 7 shows the evolution of HOM deviation from default values in the four tuning approaches. As seen in the figure, changes introduced by OE are smaller than those caused by the balancing approaches ($\overline{HOM^{(dev)}} = 4.8$ dB for OE at the end of the optimization process, against 6, 7.3 and 6.4 dB for LB, TB and EB-C, respectively). Thus, OE reaches a better network performance with less parameter changes. Less intervention over the network is an important advantage of OE, since operators are usually reluctant to modify network parameters by large amounts. OE efficiency comes directly from its analytical formulation, so that HOM is changed in the exact amount to achieve an increase in $\overline{QoE}$, and stopping when interference to/from neighbor cells becomes too high. In contrast, LB, TB and EB-C keep
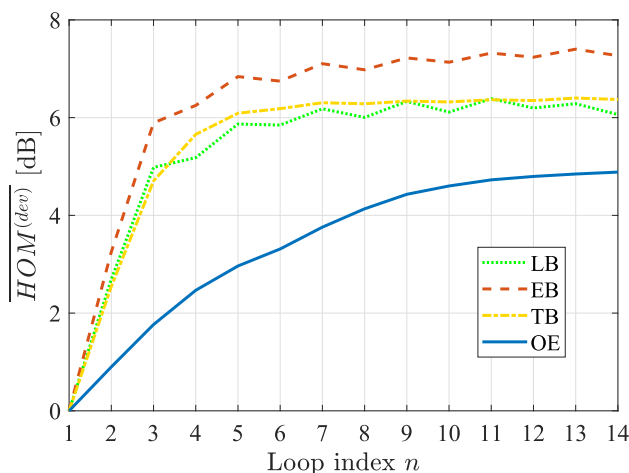
FIGURE 7. Evolution of HOM values.

enlarging underutilized cells, even if this degrades the overall system QoE.

D. IMPLEMENTATION ISSUES

The OE algorithm is executed on a per-adjacency basis. Therefore, its worst-case time complexity is $\mathcal{O}(N_{adjs})$. For the considered scenario, consisting of 108 cells and 11664 adjacencies, the average execution time of 1 iteration of OE is 4.34 minutes (22 ms per adjacency) in a personal computer with a 3.6-GHz octa-core processor and 24 GB of RAM. Runtime can be decreased by restricting changes to the closest neighbors.

V. CONCLUSION AND FUTURE WORK

In this article, a novel traffic steering algorithm for optimizing the average user QoE in a LTE network by adjusting handover margins has been proposed. The method takes a gradient ascent approach to ensure that parameter changes always improve the overall system QoE. For this purpose, the impact of parameter changes on system QoE is estimated with an analytical network performance model adjusted with statistics from the real network. Method assessment has been carried out in a dynamic system-level LTE simulator implementing a realistic macrocellular scenario considering a file download service. Results have shown that OE manages to increase the average user QoE in the network by 11.45 %, outperforming legacy balancing algorithms. Equally important, OE achieves optimal performance with smaller handover margin modifications (up to a 33 % less than other approaches). Future work will extend the proposed analytical approach to consider a multi-service scenario with delay-sensitive applications (e.g., mission critical services).

REFERENCES

[1] "Understanding smartphone behavior in the network," Nokia Siemens Networks, Espoo, Finland, White Paper, 2011.

[2] *Ericsson Mobility Report*, Ericsson AB, Stockholm, Sweden, Nov. 2017.

[3] *Technical Report; The Benefits of SON in LTE: Self-Optimizing and Self-Organizing Networks*, Americas 4G, Bellevue, WA, USA, 2009.

[4] *Next Generation Mobile Networks Recommendation on SON and O&M Requirements*, NGMN, 2008.

[5] S. Hämäläinen, H. Sanneck, and C. Sartori, "LTE self-organizing networks (SON): Network management automation for operational efficiency hard-cover," Wiley, 2012.

[6] R. Kwan, R. Arnott, R. Paterson, R. Trivisonno, and M. Kubota, "On mobility load balancing for LTE systems," in *Proc. IEEE 72nd Veh. Technol. Conf. Fall*, Sep. 2010, pp. 1–5.

[7] P. Muñoz, R. Barco, and I. de la Bandera, "Optimization of load balancing using fuzzy Q-Learning for next generation wireless networks," *Expert Syst. Appl.*, vol. 40, no. 4, pp. 984–994, Mar. 2013.

[8] J. M. Ruiz-Avilés, S. Luna-Ramírez, M. Toril, and F. Ruiz, "Traffic steering by self-tuning controllers in enterprise LTE femtocells," *EURASIP J. Wireless Commun. Netw.*, vol. 2012, no. 1, p. 337, Nov. 2012.

[9] S. Luna-Ramírez, M. Toril, M. Fernández–Navarro, and V. Wille, "Optimal traffic sharing in GERAN," *Wireless Pers. Commun.*, vol. 57, no. 4, pp. 553–574, Apr. 2011.

[10] A. J. Fehske, H. Klessig, J. Voigt, and G. P. Fettweis, "Concurrent load-aware adjustment of user association and antenna tilts in self-organizing radio networks," *IEEE Trans. Veh. Technol.*, vol. 62, no. 5, pp. 1974–1988, Jun. 2013.

[11] J. Kojima and K. Mizoe, "Radio mobile communication system wherein probability of loss of calls is reduced without a surplus of base station equipment, U.S. Patent 4435840," , vol. 54, no. 5, pp. 1875–1886, Sep. 1984.

[12] V. Bratu and C. Beckman, "Base station antenna tilt for load balancing," in *Proc. 7th Eur. Conf. Antennas Propag. (EuCAP)*, Jan. 2013, pp. 2039–2043.

[13] Y. Khan, B. Sayrac, and E. Moulines, "Centralized self-optimization in LTE–A using active antenna systems," in *Proc. IFIP Wireless Days (WD)*, Nov. 2013, pp. 1–3.

[14] N. Papaoulakis, D. Nikitopoulos, and S. Kyriazakosin, "Practical radio resource management techniques for increased mobile network performance," in *Proc. 12th IST Mobile Wireless Commun. Summit*, Jun. 2003.

[15] P. Munoz, R. Barco, I. de la Bandera, M. Toril, and S. Luna-Ramirez, "Optimization of a fuzzy logic controller for handover-based load balancing," in *Proc. IEEE 73rd Veh. Technol. Conf. (VTC Spring)*, May 2011, pp. 1–5.

[16] V. Wille, S. Pedraza, M. Toril, R. Ferrer, and J. Escobar, "Trial results from adaptive hand-over boundary modification," *IEE Electron. Lett.*, vol. 39, pp. 405–407, Feb. 2003.

[17] G. Gómez, J. Lorca, R. García, and Q. Pérez, "Towards a QoE-driven resource control in LTE and LTE—A networks," *J. Comput. Netw. Commun.*, vol. 2013, pp. 1–15, Jan. 2013.

[18] P. Oliver-Balsalobre, M. Toril, S. Luna-Ramírez, and J. M. Ruiz Avilés, "Self-tuning of scheduling parameters for balancing the quality of experience among services in LTE," *EURASIP J. Wireless Commun. Netw.*, vol. 2016, no. 1, p. 7, Jan. 2016.

[19] M. L. Mari-Altozano, S. Luna-Ramirez, M. Toril, and C. Gijon, "A QoE-driven traffic steering algorithm for LTE networks," *IEEE Trans. Veh. Technol.*, vol. 68, no. 11, pp. 11271–11282, Nov. 2019.

[20] C. Gijon, M. Toril, S. Luna-Ramirez, and M. Luisa Mari-Altozano, "A data-driven traffic steering algorithm for optimizing user experience in multi-tier LTE networks," *IEEE Trans. Veh. Technol.*, vol. 68, no. 10, pp. 9414–9424, Oct. 2019.

[21] P. A. Sánchez, S. Luna-Ramírez, M. Toril, C. Gijón, and J. L. Bejarano-Luque, "A data-driven scheduler performance model for QoE assessment in a LTE radio network planning tool," *Comput. Netw.*, vol. 173, May 2020, Art. no. 107186.

[22] M. Toril and V. Wille, "Optimization of handover parameters for traffic sharing in GERAN," *Wireless Pers. Commun.*, vol. 47, no. 3, pp. 315–336, Feb. 2008.

[23] J. L. Bejarano-Luque, M. Toril, M. Fernandez-Navarro, R. Acedo-Hernandez, and S. Luna-Ramirez, "A data-driven algorithm for Indoor/Outdoor detection based on connection traces in a LTE network," *IEEE Access*, vol. 7, pp. 65877–65888, 2019.

[24] P. Oliver-Balsalobre, M. Toril, S. Luna-Ramirez, and R. G. Garaluz, "Self-tuning of service priority parameters for optimizing quality of experience in LTE," *IEEE Trans. Veh. Technol.*, vol. 67, no. 4, pp. 3534–3544, Apr. 2018.

[25] C. Chandra, T. Jeanes, and W. H. Leung, "Determination of optimal handover boundaries in a cellular network based on traffic distribution analysis of mobile measurement reports," in *Proc. IEEE 47th Veh. Technol. Conf. Technol. Motion*, May 1997, pp. 305–309.

[26] J.-H. Rhee, J. M. Holtzman, and D.-K. Kim, "Scheduling of real/non-real time services: Adaptive EXP/PF algorithm," in *Proc. 57th IEEE Semiannu. Veh. Technol. Conf., VTC -Spring.*, Apr. 2003, pp. 462–466.

[27] L. C. Gimenez, I. Z. Kovacs, J. Wigard, and K. I. Pedersen, "Throughput-based traffic steering in LTE-advanced HetNet deployments," in *Proc. IEEE 82nd Veh. Technol. Conf. (VTC-Fall)*, Sep. 2015, pp. 1–5.

MARÍA LUISA MARÍ ALTOZANO received the M.S. degree in telecommunication engineering from the University of Málaga, Spain, in 2012, where she is currently pursuing the Ph.D. degree with the Department of Communication Engineering. From 2013 to 2016, she was with Ericsson in a collaborative project with the University of Málaga. Her research interest includes self-optimization of mobile radio access networks based on quality of experience.

MATÍAS TORIL received the M.S. degree in telecommunication engineering and the Ph.D. degree from the University of Málaga, Spain, in 1995 and 2007, respectively. Since 1997, he has been a Lecturer with the Department of Communications Engineering, University of Málaga, where he is currently a Full Professor. He has authored more than 110 publications in leading conferences and journals and three patents owned by Nokia Corporation. His current research interests include self-organizing networks, radio resource management, and data analytics.

SALVADOR LUNA-RAMÍREZ (Member, IEEE) received the M.S. degree in telecommunication engineering and the Ph.D. degree from the University of Málaga, Spain, in 2000 and 2010, respectively. Since 2000, he has been with the Department of Communications Engineering, University of Málaga, where he is currently an Associate Professor. His research interests include self-optimization of mobile radio access networks and radio resource management.

CAROLINA GIJÓN received the B.S. degree in telecommunication systems engineering from the University of Málaga, Spain, in 2016. She is currently pursuing the Ph.D. degree. Her research interests include self-organizing networks and radio resource management.

● ● ●